Amplification of Microwave Magnetic Envelope Solitons in Thin Yttrium Iron Garnet Films by Parallel Pumping

Pavel A. Kolodin,* Pavel Kabos,† and Carl E. Patton
Department of Physics, Colorado State University, Fort Collins, Colorado 80523

Boris A. Kalinikos, Nikolai G. Kovshikov, and Mikhail P. Kostylev
St. Petersburg Electrotechnical University, 197376, St. Petersburg, Russia
(Received 10 July 1997)

The parametric amplification of 4.01 GHz, 22 ns wide microwave magnetic envelope (MME) backward volume wave pulses by parallel pumping has been realized in yttrium iron garnet (YIG) films. The parametric parallel pumping was achieved with 15–23 ns wide pulses applied to a strip line resonator at a frequency ω_p approximately twice the signal frequency ω_s. Low power linear MME pulse signals were pumped to form solitons with a gain of 20 dB, and soliton signals could be boosted by 8 dB. These large gain factors occur only when ω_p is upshifted from $2\omega_s$ by 30 MHz. This upshift is critical and is related to the nonlinear nature of the soliton signal. [S0031-9007(98)05461-1]

PACS numbers: 75.30.Ds, 76.50.+g, 85.70.Ge

Nonlinear excitations in the form of microwave magnetic envelope (MME) solitons have become a subject of growing interest [1,2]. The capability of solitons to preserve their shape during propagation makes these excitations promising for fundamental work in nonlinear science as well as various signal processing applications. Dissipation plays a significant role in limiting the propagation of these MME solitons. Typically, the rate of decay is found to be faster for soliton than for linear wave packets [1]. Even for high quality low loss yttrium iron garnet (YIG) films, the decay times for single soliton propagation are on the order of 100 ns or less and useful propagation distances are typically below one cm or so.

It is desirable, therefore, to provide some way to amplify these MME pulses to compensate for the loss and thereby obtain longer soliton propagation times and distances. One of the well-known amplification mechanisms for magnetostatic waves (MSW) is the parallel pumping [3] process when the static magnetic field and the high frequency magnetic field are parallel. It has been demonstrated that the amplification of MSW signals in thin ferromagnetic films by parallel pumping is possible [4,5]. Recent measurements on the parallel pumping of MSW solitons have shown a modest pulse enhancement of 1.4 dB [6]. However, a recent theoretical analysis suggests that the gain could be considerably higher [7].

This Letter reports a new and highly effective way to parametrically pump MME linear wave packets and solitons to produce significant gain. This technique does more than provide some limited compensation for decay due to dissipation. It leads to a real amplification of the propagating signal. Further, it is demonstrated for the first time that parallel parametric pumping can be used to form a soliton from a linear MME pulse. One can, therefore, begin with an MME soliton after decay into a linear pulse, and reshape the signal back to the soliton state.

Figure 1 shows the YIG film and the microstrip transducer structure used for the experiments. The experiments utilized an epitaxial single-crystal YIG film strip, 4.9 μm thick, 20 mm long, and 1.6 mm wide. The parent film was grown on a gadolinium gallium garnet (GGG) substrate by standard liquid phase epitaxy techniques. The half-power ferromagnetic resonance linewidth of the film was 0.6 Oe at 4 GHz. Under the center part of the film strip, one has 50 μm wide input and output transducers spaced 8.5 mm apart. An in-plane static magnetic field of 784 Oe is applied parallel to the long edge of the film strip in the magnetostatic backward volume wave (MSBVW) configuration. At this field, the MSBVW passband had a measured upper limit band edge frequency of 4.076 GHz. The MME input pulse carrier signal frequency ω_s was chosen to be 4.01 GHz, 66 MHz below this band edge. This corresponds to an operating point wave number of about 200 rad/cm.

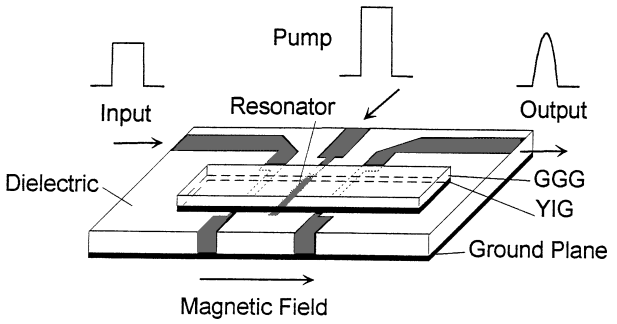

FIG. 1. Diagram of the yttrium iron garnet (YIG) film and transducer structure setup. The structure consists of two 50 μm wide microstrip transducers and a 0.25 mm wide microstrip pumping resonator on a single ground plane dielectric substrate. The YIG film on a gadolinium gallium garnet (GGG) substrate was placed across the transducers, with input, output, and parametric pumping signals as indicated. The static magnetic field was parallel to the propagation direction.

 0031-9007/98/80(9)/1976(4)$15.00

The parallel pumping microwave field was applied by a half wavelength long 0.25 mm wide microstrip resonator between the input and output transducers at the distance of 4 mm from the input transducer. The resonator was pumped at a frequency $\omega_p = 8.05$ GHz. The long edge of the resonator was parallel to the input and output transducers, and the resonator was positioned precisely under the center of the YIG film. For this geometry, the microwave magnetic field of the resonator is mostly parallel to the static magnetic field. This defines the parallel pumping geometry. A second structure with a movable output transducer was used to monitor the MME pulse signal at the position of the resonator.

The 22 ns wide input pulses at $\omega_s = 4.01$ GHz were launched from the input transducer. The measured MME pulse group velocity v_g was 2.15×10^6 cm/s, for a delay of 180 ns at the position of the resonator. At precisely this time after launch, the pumping pulse at $\omega_p = 8.05$ GHz was applied to the resonator. Note that ω_s is 15 MHz below $\omega_p/2$. A signal frequency which is 15 MHz lower than one-half the pump frequency was found to produce the highest gain. At $\omega_s = 4.01$ GHz, the pulse signal power spectrum for solitons has an additional peak at 4.025 GHz, which is precisely half the pump frequency needed for maximum gain. There is a clear connection between high parametric gain and this shifted peak in the nonlinear signal power spectrum.

The effects of the pumping on propagating MSBVW pulses at two different input power levels are shown by the input and output power vs time data in Fig. 2. For the graph in Fig. 2(a), the input power of 50 mW was high enough to produce a soliton at the resonator position. The dashed line at 200 ns shows this signal as measured with structure No. 2. Further propagation without pumping gave the small dashed signal at 400 ns. Parallel pumping with a 15 ns wide, 5 W resonator pulse caused the increase in the output signal shown by the solid curve at 400 ns. The increase amounts to a gain of 4.5 dB. The 15 ns pump pulse width was approximately equal to the width of the soliton pulse at the resonator position. These data demonstrate the effect of the parametric pumping in boosting the soliton amplitude.

Figure 2(b) is for an input pulse power of 4 mW which was well below the soliton regime. The format is the same as for Fig. 2(a). Here, the resonator pulse width was 23 ns to match the dispersed input pulse width at the resonator position under these low power conditions. Figure 2(b) shows that the effect of the parametric pumping on the signal pulse is much bigger under low power conditions. The increase in peak power here is about 15 dB. It is important to note that the large amplitude output pulse in Fig. 2(b) is a soliton. The parallel pumping has boosted the low power MME pulse up to soliton status. Further data on this result will be presented shortly.

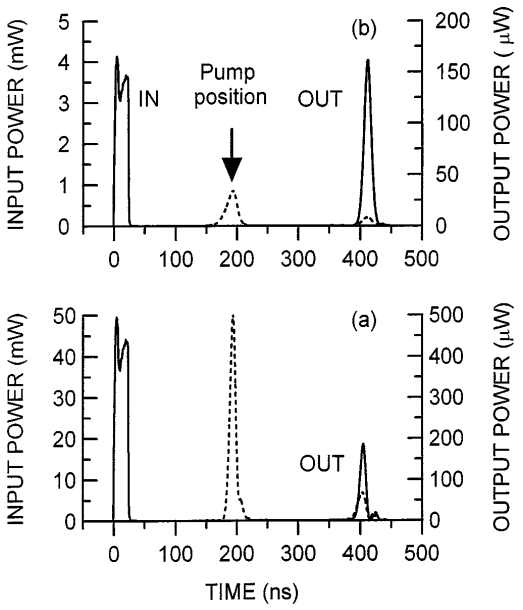

FIG. 2. Representative pulse data with and without parametric pumping. The 4.01 GHz input pulse was 22 ns wide. The resonator pulse was at 8.05 GHz and 5 W. The dashed lines at 200 ns show the MME pulse profile at the resonator position. The dashed pulses at 400 ns show the output signals without pumping. The solid line pulses at 400 ns show the output signal with pumping. For (a) the input pulse power was 50 mW and the resonator pulse width was 15 ns. For (b) the input pulse power was 4 mW and the resonator pulse width was 23 ns.

It is important to emphasize that the resonator pulse timing is critical. Experiments with long pumping pulses showed that if the resonator pulse starts well before the MME pulse reaches the resonator position, there will be a very rapid decrease in the amplification. This demonstrates clearly and unambiguously that the parametric amplification process starts immediately after pumping is turned on. This effect is consistent with the recently published results of Bagada *et al.* [6] which report a maximum parametric gain of 1.4 dB for a pump pulse of long duration which is switched on several hundred nanoseconds before the signal pulse reaches the pumping zone. No reason for this delay is given. It appears that the delay in [6] actually reduces the realizable gain.

Figure 3 shows output pulse data corresponding to the graph of Fig. 2(b) in more detail. Figures 3(a) and 3(b) show the MME pulse amplitude profiles at the output transducer with and without a resonator pulse, respectively. Figures 3(c) and 3(d) show phase profiles which correspond to Figs. 3(a) and 3(b). The low amplitude profile in Fig. 3(a) represents the low power MME pulse at the output transducer. This pulse has experienced both decay and dispersion. Figure 3(c) shows a typical phase profile for such a dispersed pulse with a concave downward character. The poor signal to noise for Fig. 3(c) is due to the lower power level.

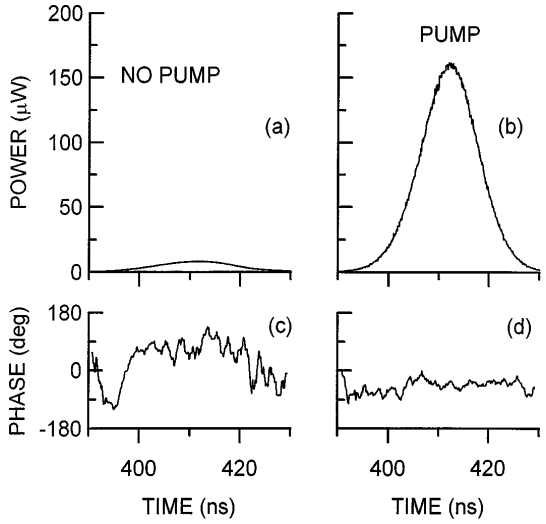

FIG. 3. Expanded view of output pulse profiles from Fig. 2(b). Graphs (a) and (b) show the output pulses with no resonator pulse and with the resonator pulse, respectively, the same as the dashed and solid line curves at 400 ns in Fig. 2(b). Graphs (c) and (d) show phase profiles corresponding to (a) and (b), respectively.

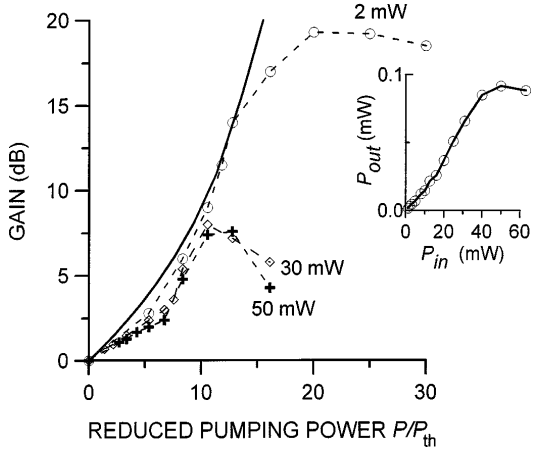

FIG. 4. Output pulse gain due to the resonator parallel pumping as a function of the resonator power P divided by the cw parallel pump threshold P_{th} for three different input pulse powers as indicated. The inset shows the output peak power P_{out} vs input power P_{in} response with no resonator power applied.

The boosted output amplitude profile in Fig. 3(b) has a significantly different companion phase profile. Figure 3(d) shows a phase profile which is essentially constant. A constant phase profile is one critical signature of an MME soliton [2]. Figure 2(b) and Figs. 3(b) and 3(d) demonstrate the effect of the parallel pumping to actively boost and reshape the dispersive linear low power MSBVW pulse into a soliton. It is important to emphasize the significance of this result. The localized parallel pumping results not only in 15 dB of amplification, but also in the formation of a MME soliton from a low amplitude linear pulse.

The results shown above are for one nominal value of the pumping power applied to the resonator. Measurements of the gain due to the parametric pumping were also made as a function of the resonator pulse power. It was found that the pumping power had to be at least several times the cw parallel pumping threshold power level P_{th} for the resonator in order to obtain any gain from the parametric pump. This threshold was measured in two ways: (1) from measurements of the signal reflected from the resonator under cw excitation as a function of the power applied to the resonator, and (2) from measurements of the parametric MSW signal at the output transducer as a function of the cw resonator power. Both methods gave $P_{\text{th}} = 0.18$ W.

Figure 4 shows the results of these additional measurements of the output signal amplitude as a function of the resonator pumping power for three different input pulse power levels. Pumping pulse width for all three cases was 23 ns. The graph shows the signal gain factor in dB as a function of the resonator power P divided by P_{th}. The three sets of measurements shown by the data points and dashed lines are for three input power levels, as indicated. The solid curve shows a theoretical result to be discussed shortly. The inset shows the output peak power P_{out} vs input power P_{in} response for the MSBVW pulses with no resonator pumping.

The 2, 30, and 50 mW P_{in} levels for the measurements in Fig. 4 represent three different propagation regimes. The 2 mW level corresponds to a linear response near the origin of the inset graph. Here, the MSBVW propagation is dispersive, and there is no soliton formation. The 30 mW input level is close to the inflection point of the inset response curve. Here, there is single soliton formation. The 50 mW level is close to the maximum response point in the inset and corresponds to the beginning of multisoliton formation.

As the data in Fig. 4 show, the parametric pumping in the low power linear regime with $P_{\text{in}} = 2$ mW produces the largest gain. The gain at $P/P_{\text{th}} \approx 20$ is nearly 20 dB. Recall from the above discussion that this regime corresponds to the parametric pumping conversion of a linear MSBVW pulse into a high amplitude soliton.

As the input power is increased, the gain drops rapidly and the peak gain shifts to a factor of 2 lower P/P_{th} ratio. The drop in gain with increased resonator power is related to the formation of higher order solitons and the related decrease in the soliton peak power [1]. This effect was clearly demonstrated through the appearance of additional peaks in the output signal profiles. It is important to note that the normalized gain curves for $P_{\text{in}} = 30$ mW and $P_{\text{in}} = 50$ mW are virtually identical. These data represent saturation gain curves for the parametrically pumped soliton signals.

The parallel pumping process which is responsible for the highly efficient amplification process discovered

here has been analyzed very recently by Kalinikos and Kostylev [7]. The high power pump at ω_p drives two transient nonresonant idler waves in the YIG pumping zone around the microstrip resonator. The nonlinear interaction between these idler waves and the MME pulse yields amplification. The amplification process is active only during the transient growth of the idler signals and *before* the onset of the parametric generation of spin waves by the pump. The amplification process is *not* due to the parametric excitation of spin waves by the pumping signal. The full theory in [7] yields a gain coefficient for a spectrally narrow MME signal propagated through a parallel pump zone of width L which may be written as

$$G = \frac{\kappa v_g}{\eta \sinh(\kappa L) + \kappa v_g \cosh(\kappa L)}, \quad (1)$$

where η is the relaxation rate and κ is an increment given by

$$\kappa = \frac{\sqrt{\eta^2 - h^2 V^2}}{v_g}. \quad (2)$$

Here h is the amplitude of the microwave pumping field, and V is a parallel pump coupling parameter. For MSBVW signals, V is given by

$$V = \frac{|\gamma| 4\pi M_s}{8\omega} \frac{1}{kd}(1 - e^{-kd}), \quad (3)$$

where d is YIG film thickness and k is MSBVW wave number. For the resonance linewidth cited above, the 4 GHz relaxation rate η is 5.28×10^6 rad/s.

Equation (1) is based on a parallel pump microwave field which is strictly bounded to a region of width L. The microwave field in the YIG film from the resonator has a somewhat more complicated geometry. The L parameter, therefore, was taken as an effective width for the experimental pumping zone and treated as an adjustable parameter. The value of L required to produce the solid curve in Fig. 4, in combination with the cited values of the other parameters, was 2.3 mm. While this value is significantly larger than the width of the resonator, a few mm is a reasonable value for the spatial extent of the microwave magnetic field. The theoretical fit matches the data reasonably well, as long as one stays below the power regime for multisoliton effects.

This work was supported in part by the U.S. Army Research Office, Grant No. DAAH04-95-1-0325, the National Science Foundation, Grant No. DMR-9400276, the Russian Foundation for Basic Research, Grant No. 96-02-19515, the Slovak Science Foundation, Grant No. 1/4288/97, and the NATO Linkage Grant Program, Grant No. HTECH.LG 970538.

*Permanent address: St. Petersburg Electrotechnical University, 197376 St. Petersburg, Russia.

†On leave from the Slovak Institute of Technology, Bratislava, Slovakia.

[1] See N. G. Kovshikov, B. A. Kalinikos, C. E. Patton, E. S. Wright, and J. Nash, Phys. Rev. B **54**, 15 210 (1996), and references therein.

[2] B. A. Kalinikos, N. G. Kovshikov, and E. E. Patton, Phys. Rev. Lett. **78**, 2827 (1997).

[3] E. Schlömann, J. J. Green, and U. Milano, J. Appl. Phys. **31**, 386S (1960).

[4] B. A. Kalinikos, M. K. Kovaleva, and N. G. Kovshikov, Avtorskoe Svidetel'stvo, USSR Patent No. 778606, (1979), published in Izobreteniya I Otkrytiya, No. 26, p. 225 (1988).

[5] G. A. Melkov and S. V. Sholom, Zh. Tekh. Fiz. **60**, 118 (1990) [Sov. Phys. Tech. Phys. **35**, 943 (1990)].

[6] A. V. Bagada, G. A. Melkov, A. A. Serga, and A. N. Slavin, Phys. Rev. Lett. **79**, 2137 (1997).

[7] B. A. Kalinikos and M. P. Kostylev, IEEE Trans. Magn. **33**, 3445 (1997).